ISSN NO. 2320-5407

Journal homepage: http://www.journalijar.com

INTERNATIONAL JOURNAL OF ADVANCED RESEARCH

RESEARCH ARTICLE

Employing Cyclic Stress for Studying Corrosion and Corrosion Inhibition of C-Steel in Aqueous Solutions

[*]Hala.M.Hassan[1], A.M.Eldesoky[2], A.S.Fouda[3]

1.Textile Technology Department, Industrial Education College, Beni-Suef University, Egypt and Chemistry Department, Faculty of Science, Jazan University, KSA

2.Engineering Chemistry Department, High Institute of Engineering & Technology (New Damietta), Egypt and Al-Qunfudah Center for Scientific Research (QCSR), Al-Qunfudah University College, Umm Al-Qura University, KSA.

3. Department of Chemistry, Faculty of Science, El-Mansoura University, El-Mansoura-35516, Egypt

Manuscript Info

Manuscript History:

Received: 12 February 2014
Final Accepted: 22 March 2014
Published Online: April 2014

Key words:
Cyclic Stress, C-steel, Frumkin, Quantum Calculations

Corresponding Author

Hala.M.Hassan

Abstract

The inhibitive effect of some organic derivatives on the corrosion of cyclic stressed C-steel specimens in 2 M HCl in the presence of organic derivatives with concentrations (1×10^{-6} M – 11×10^{-6} M) at 30 ^{o}C was studied using galvanostatic polarization, and weight loss techniques. The inhibiting effect was attributed to the adsorption of the additives on the C- steel surface. The data obtained fit well to Frumkin adsorption isotherm. The results of polarization studies indicate that the investigated organic derivatives are mixed type inhibitors. The presence of the inhibitors with the aggressive solution 2 M HCl improves of the relative reduction of fatigue life of the C-steel. The presence of the studied compounds solution inhibits both the hydrogen evolution and the anodic dissolution processes with overall shift of E_{corr} to more negative values with respect to the OCP. The increase in the inhibition efficiency of investigated inhibitors with the addition of iodide ions indicates that iodide ions play important role in the adsorption process. The efficiencies obtained from the three different techniques were in good agreement which prove the validity of these tools in the measurements of the tested inhibitors.

1. Introduction

Corrosion is a fundamental process playing an important role in economics and safety, particularly for metals and alloys. Steel has found wide applications in a broad spectrum of industries and machinery; despite its tendency to corrosion. Corrosion inhibition of steel, therefore is a matter of theoretical as well as practical importance [1–8]. Acid solutions are widely used in industry, some of the important fields of applications being acid pickling of iron and steel, chemical cleaning and processing, ore production and oil well acidification. Because of the aggressiveness of acid solutions, inhibitors are commonly used to reduce the corrosive attack on metallic materials. Most well-known acid inhibitors are organic compounds containing nitrogen, sulfur, and oxygen atoms. However, these compounds, despite their high inhibition performance, are toxic and carcinogenic. The safety and environmental issues of corrosion inhibitors arisen in industries has always been a global concern. However, only a few non-toxic and eco-friendly compounds have been investigated as corrosion inhibitors. Amino acids are environmentally friendly compounds. In addition, amino acids are from a class of organic compounds, completely soluble in aqueous media. These properties would justify their use as corrosion inhibitors. Some recent studies involving amino acids on the corrosion of iron and steel were reported [9–13]. Experimental means are useful in explaining the inhibition mechanism, but they are often expensive and time-consuming. Advances in computer hardware and software and in theoretical chemistry have brought high-performance computing and graphic tools within the reach of many academic and industrial laboratories.

Recently, a program is in progress in our lab to present substantial quantum chemical calculations in our corrosion publications [14–17]. Such calculations are usually used to explore the relationship between the inhibitor molecular properties and their corrosion inhibition efficiencies.

This study aims to gain some insight into the corrosion of C-steel in HCl in the presence and absence of some organic derivatives as inhibitors using chemical and electrochemical techniques. Additionally, thermodynamic data were obtained from adsorption isotherms and Arrhenius plots. These organic derivatives were chosen as corrosion inhibitors due to: (a) higher molecular size (b) π-electron contribution of the benzene rings and (c) presence of more active adsorption sites. It was also the purpose of the present work to discuss the relationship between quantum chemical calculations and experimental protection efficiencies of the series two of inhibitors (Thiazolidin-5-one derivatives) by determining various quantum chemical parameters. These parameters include the highest occupied molecular orbital (E_{HOMO}) and the lowest unoccupied molecular orbital (E_{LUMO}), the energy difference (ΔE) between E_{HOMO} and E_{LUMO}. Also the inhibition effect of the organic derivatives on the corrosion fatigue (CF) of C-steel specimens stressed by cyclic stress with cyclic frequency of 10.5 Hz while immersed in hydrochloric acid solution is assessed by using in situ measurements of electrochemical galvanostatic polarization.

2. Experimental Methods

2.1. Materials and Specimens

Table (1): Chemical Composition (wt%) of the Carbon Steel

C	Mn	P	Si	Fe
0.200	0.91	0.007	0.002	rest

Table (2): The Mechanical Properties of Carbon Steel

Yield Stress (Mpa)	Tensile Strength (Mpa)	Elongation (Lo=5do)%
335	322	19

2.2. Chemicals Additives and Solutions

2.2.1. Chemical Additives

a. Hydrochloric acid. (BDH grade)

b. Organic additives

The organic additives which used inhibitors in this study were listed below [18]:

Series One

(I)

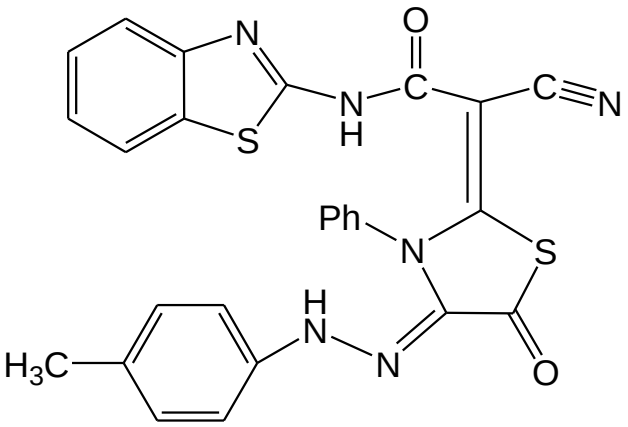

(2*E*)-2-((*Z*)-4-(2-*p*-tolylhydrazono)-5-oxo-3-phenylthiazolidin-2-ylidene)-*N*-(benzo[*d*]thiazol-2-yl)-2-cyanoacetamide

(II)

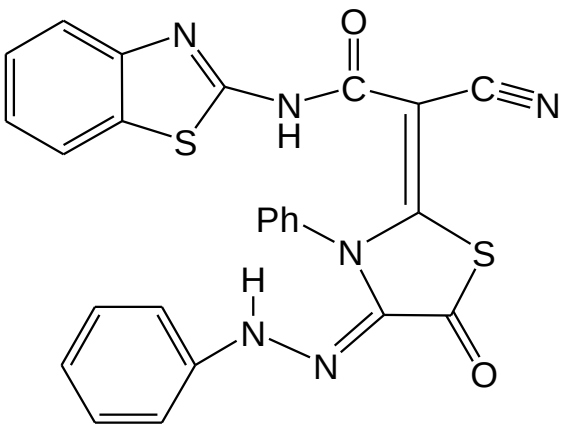

(2*E*)-2-((*Z*)-4-(2-phenylhydrazono)-5-oxo-3-phenylthiazolidin-2-ylidene)-*N*-(benzo[*d*]thiazol-2-yl)-2-cyanoacetamide

(III)

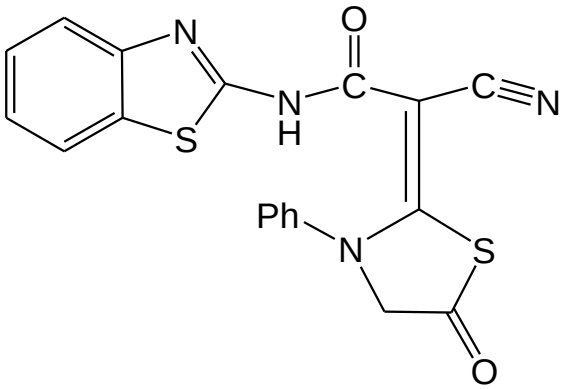

(*E*)-*N*-(benzo[*d*]thiazol-2-yl)-2-cyano-2-(5-oxo-3-phenylthiazolidin-2-ylidene)acetamide

Series Two

(IV)

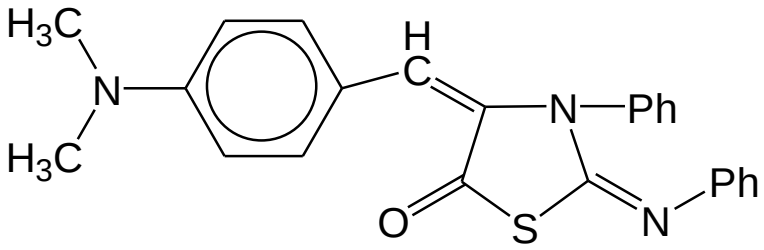

(2*E*,4*E*)-4-(4-(dimethylamino)benzylidene)-3-phenyl-2-(phenylimino)thiazolidin-5-one

(V)

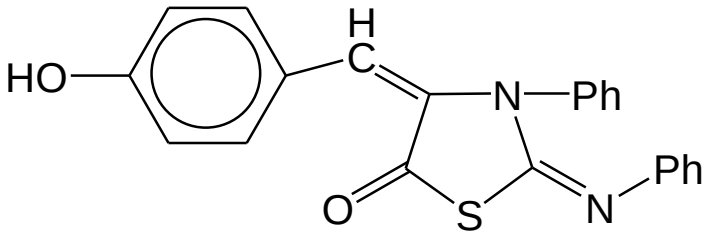

(2*E*,4*E*)-4-(4-hydroxybenzylidene)-3-phenyl-2-(phenylimino)thiazolidin-5-one

(VI)

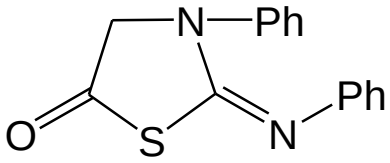

(*E*)-3-phenyl-2-(phenylimino)thiazolidin-5-one

c. Inorganic Additives

The inorganic additive used in this study is KI, (BDH grade).

2.2.2 Solutions

a. Hydrochloric Acid Solution

Approximately 2 M hydrochloric acid solutions were prepared by diluting the appropriate volume of the concentrated chemically pure grade acid (BDH), with double distilled water. The concentrations of the acid were checked by titration of an appropriately diluted portion with standard solution of sodium carbonate. From this stock, concentrated solutions exactly 2 M HCl were prepared by dilution with double distilled water, which was used throughout experiments for the preparation of solutions**.**

b. Inhibitors Solution

100 ml stock solutions (10^{-2} M) of the compounds were prepared by dissolving an accurately quantity of each material in the appropriate volume of ethanol, then the required concentrations ($1x10^{-6}$ - $11x10^{-6}$) were prepared by dilution with doubly distilled water**.**

c. Inorganic Additives Solutions

100 ml stock solutions (1 M) of the salt (BDH grade) were prepared by dissolving an accurately quantity of each material in the appropriate volume of doubly distilled water, from these stock solutions exactly $1x10^{-2}$ M KI was prepared by dilution with doubly distilled water.

2.3. Experimental Techniques

2.3.1. Electrochemical Technique (Galvanostatic Polarization Method)

a. Electrodes

Chemical composition of C-steel used in this study is given in Table (1). Two different types of electrodes were used; disks with 12 mm diameter and 2 mm thickness and cylindrical specimens. The discs were welded from one side to a copper wire for electric connection and embedded in glass tube of larger diameter than the sample. Epoxy resin was used to stick the sample to the glass tube except the exposed tested surface area which was left to be exposed to the corrosive media.

Cylindrical specimens were used in the fatigue test and in electrochemical measurements after fatigue test in air. The specimen diameter was 10 mm while the gage length of the middle part was 20 mm and its diameter was 4 mm, and the overall length was 140 mm as shown in Fig. (1). The gage length of all specimens were prepared by treatment with emery papers n. 1000, then degreased in acetone ultrasonic bath, washed with bi-distilled water and dried.

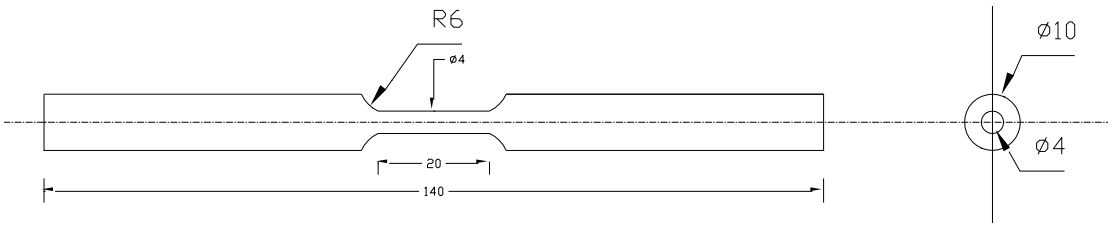

Fig. (1): Specimen of Fatigue Test (Dim. mm)

Fatigue tests were performed at 10.5 Hz on a cantilever rotary-bending fatigue test machine, with different cyclic stress (82 MPa – 247 MPa) and number of cycles (63000). The specimens were coated with epoxy resin except the test section that immersed in the solution during the entire galvanostatic polarization test. The corrosive media used was 2 M HCl. Solutions containing (1×10^{-6} M - 11×10^{-6} M) organic derivatives were used as inhibitors.

2.3.2. Chemical Technique (Weight Loss Method)

The reaction basin was graduated glass vessel 6 cm inner diameter and having a total volume of 250 ml. 100 ml of the test solution were employed in each experiment. The test pieces were cut into 2×2×0.2 cm. They were mechanically polished with emery paper (a coarse paper was used initially and then progressively finer grades were employed), rinsed with double distilled water and finally dried between two filter papers and weighed. The test pieces were suspended by suitable glass hooks at the edge of the basin, and under the surface of the test solution by about 1 cm. After specified periods of time, 3 test pieces were taken out of the test solution, rinsed with double distilled water, dried as before and weighed again. The average weight loss at a certain time for each set of three samples was taken. The weight loss was recorded to the nearest 0.0001 g.

3. Results and Discussion

3.1. Electrochemical Measurement

Galvanostatic polarization studies were carried out on C-steel in 2 M HCl solution without and with different concentrations of the inhibitors. The tested specimen was used as working electrode. Saturated calomel electrode (SCE) was used as reference electrode while platinum wire as a counter electrode. All experiments were carried out at 25^{o}C. The inhibition efficiency (% IE) is defined as [19]:

$$\% IE = ((i_{corr.} - i_{inh.}) / i_{corr}) \times 100 \quad (1)$$

Where $i_{corr.}$ and $i_{inh.}$ are the corrosion current density in the absence and presence of inhibitors respectively. The degree of surface area coverage (θ) can be calculated from the relation:

$$\theta = (i_{corr.} - i_{inh.}) / i_{corr.} \quad (2)$$

3.1.1. Polarization Curves

Corrosion behavior of C-steel is studied in 2 M HCl solutions in absence and presence of (1×10^{-6} – 11×10^{-6}) M inhibitors (I –VI) at 25 ^{o}C. Fig. (2) show the galvanostatic polarization curve of C-steel in 2 M HCl in absence and presence of inhibitor (I) at different inhibitor concentrations, Table (3) gives the various corrosion parameters.

Tafel slopes (βa & βc) values, corrosion potential (E_{corr}), corrosion current (i_{corr}), degree of surface coverage (θ) and inhibition efficiency (% IE) indicate that:

1. The corrosion current density decreases with increasing the concentration of organic derivatives. This indicates that the presence of these derivatives retards the dissolution of C-steel in 2 M HCl solution and the degree of inhibition depends on the concentration and type of the inhibitor present.
2. The degree of surface coverage was found to increase with increasing the concentration of inhibitor.
3. The presence of the tested inhibitors retards both anodic and cathodic reactions and hence these inhibitors act as mixed type inhibitors.
4. The order of decrease in inhibition efficiency for the tested additives is:

Series 1: (I) > (II) > (III),

Series 2: (IV) > (V) > (VI)

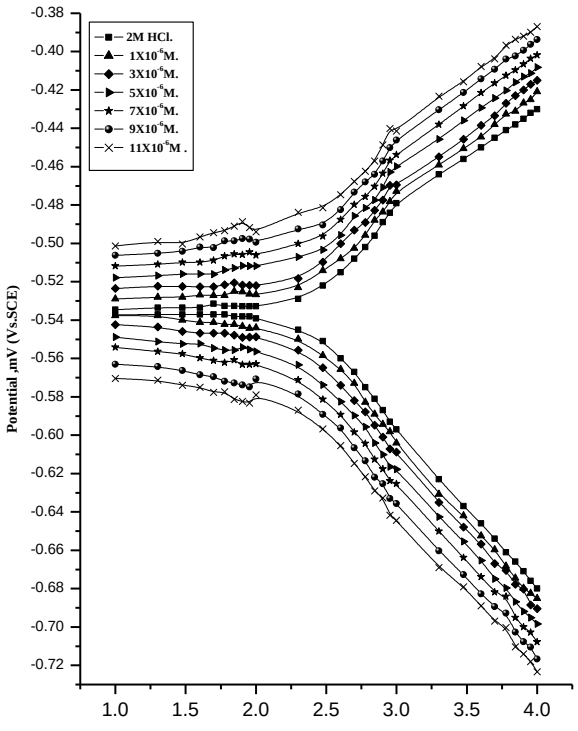

Fig.(2):Galvanostatic polarization curves of C-steel in 2M HCl in abscence and presence of inhibitor (I) at various concentrations at 25°C.

Table (3): Corrosion parameters of residual stress for C-steel in 2 M HCl at 25 °C in absence and presence at various concentrations of inhibitors (I–VI).

Inhibitors Types	Conc., M.	$-E_{corr}$ mV	$i_{corr.}$ µA cm^{-2}	β_a $mVdec^{-1}$	β_c $mVdec^{-1}$	θ	% IE
Blank	2MHCl	530	1.970	200	163	-	-
I	$1x10^{-6}$	495	0.872	189	176	0.5573	55.73
	$3x10^{-6}$	498	0.717	203	183	0.6360	63.60
	$5x10^{-6}$	502	0.699	192	179	0.6451	64.51
	$7x10^{-6}$	505	0.656	201	187	0.6666	66.66
	$9x10^{-6}$	508	0.629	208	203	0.6807	68.07
	$11x10^{-6}$	510	0.492	204	205	0.7502	75.02
II	$1x10^{-6}$	509	0.844	185	198	0.571	57.15
	$3x10^{-6}$	511	0.800	203	199	0.593	59.39
	$5x10^{-6}$	513	0.731	198	187	0.628	62.89
	$7x10^{-6}$	517	0.682	207	205	0.654	65.43
	$9x10^{-6}$	519	0.632	203	203	0.679	67.91
	$11x10^{-6}$	521	0.521	201	213	0.735	73.55
III	$1x10^{-6}$	508	0.878	201	192	0.5543	55.43
	$3x10^{-6}$	510	0.837	203	201	0.5750	57.50

	$5x10^{-6}$	515	0.801	207	203	0.5930	59.30
	$7x10^{-6}$	514	0.721	209	201	0.6340	63.40
	$9x10^{-6}$	517	0.697	206	197	0.6460	64.40
	$11x10^{-6}$	520	0.579	203	195	0.7060	70.60
IV	$1x10^{-6}$	503	0.882	202	196	0.5522	55.22
	$3x10^{-6}$	507	0.833	203	201	0.5771	57.71
	$5x10^{-6}$	509	0.773	211	213	0.6076	60.76
	$7x10^{-6}$	513	0.711	209	208	0.6390	63.90
	$9x10^{-6}$	514	0.667	214	199	0.6614	66.14
	$11x10^{-6}$	517	0.610	206	207	0.6903	69.03
V	$1x10^{-6}$	511	1.07	207	204	0.4568	45.68
	$3x10^{-6}$	517	1.031	206	201	0.4766	47.66
	$5x10^{-6}$	514	0.981	199	203	0.5020	50.20
	$7x10^{-6}$	516	0.942	203	199	0.5218	52.18
	$9x10^{-6}$	518	0.871	208	202	0.5578	55.78
	$11x10^{-6}$	519	0.782	219	210	0.6030	60.30
VI	$1x10^{-6}$	507	1.09	206	198	0.4467	44.67
	$3x10^{-6}$	509	1.038	198	203	0.4730	47.30
	$5x10^{-6}$	513	0.987	197	216	0.4989	49.89
	$7x10^{-6}$	517	0.951	203	209	0.5172	51.72
	$9x10^{-6}$	502	0.891	207	199	0.5477	54.75
	$11x10^{-6}$	498	0.793	196	207	0.5974	59.74

3.1.2. Effect of Applied Cyclic Stresses on the Corrosion Behavior of Stainless Steel 304 SS

In these experiments the measurements were carried out in 2 M HCl solution at 25 ^{o}C in absence and presence of different inhibitors at different concentrations (5×10^{-6} M – 11×10^{-6} M), while applying cyclic stresses (82 Mpa - 247 Mpa) with number of cycles (63000) at 10.5 Hz. The galvanostatic polarization curves were plotted for each inhibitor. In the rotating cantilever bending fatigue test, the tension and compression cyclic stresses occur at the outer surfaces of the specimen, for this reason plastic deformation commonly occurs by the slip of one plane over the other. Such slip is very non-uniform within a polycrystalline solid and can occur on only some of the crystal planes within a metal grain. Stressed C-steel surfaces by the rotating cantilever bending fatigue test, contain iron atoms that are more reactive hence they have a less stable crystalline environment and more susceptible to attack. Whenever a metal is stressed, the metallic crystal lattice becomes severely strained and tends to become more anodic, hence they travel into solution more readily than the atoms in less strained sites. Consequently, corrosion of the most strained regions of a metal have the highest rate of corrosion.

The polarization curves were plotted for each inhibitor as shown in Fig. (3). The results indicate that, the inhibition efficiency of inhibitors (I –VI) for the corrosion of C-steel in the acidic solution at 25 ^{o}C is decreased in order Series 1: (I) > (II) > (III) and Series 2: (IV) > (V) > (VI) with increasing the concentration of inhibitors and decreased with increasing applied cyclic stresses as shown in Table (4). The corrosion of the most strained regions of the tested specimens is most rapid, also the adsorbed layer of inhibitor on C-steel surface becomes less stable and the corrosive

media becomes more aggressive. Inspection of Tafel slopes values and E_{corr} values under these conditions indicate that these inhibitors act as mixed–type inhibitors. Also, the corrosion current density i_{corr} increased with increasing the applied cyclic stresses. The increase in the applied cyclic stress adds to the free energy of the strained atoms and hence more atoms go to the solution causing a pronounced

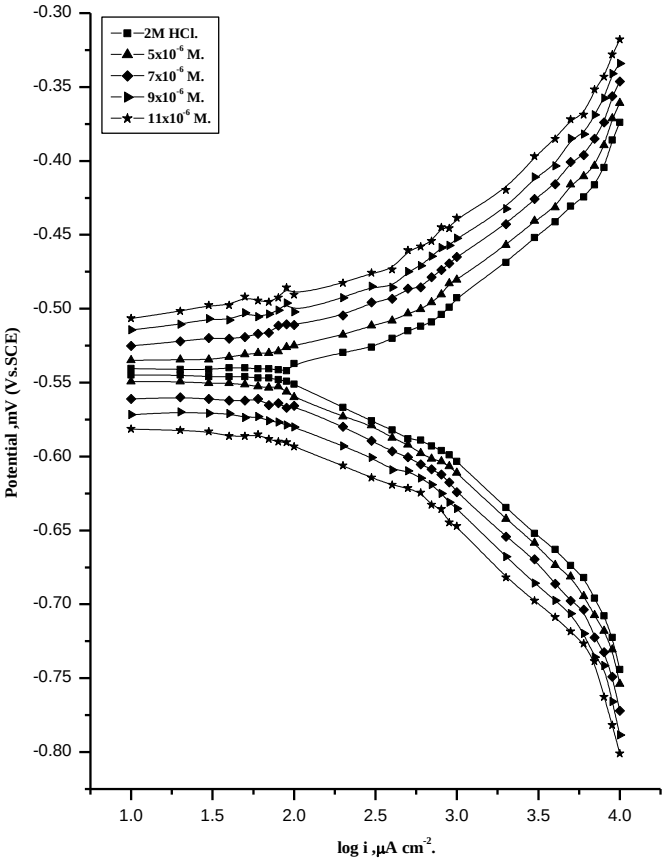

Fig.(3):Galvanostatic polarization curves of dissolution of stressed C-steel with 247 Mpa in 2M HCl in absence and presence of different concentrations of inhibitor(I) at 25°C.

Table (4): Corrosion parameters for C-steel in 2 M HCl in absence and presence of different concentrations of inhibitors (I-VI) for stressed specimens by 247 Mpa, at 63000 cycles at 30 ^{0}C.

Inhibitors Types	Conc., M.	$-E_{corr}$ mV	$i_{corr.}$ μA cm^{-2}	β_a $mVdec^{-1}$	β_c $mVdec^{-1}$	θ	% IE
Blank	2 M HCl	546	4.152	184	149	-	-
I	$5x10^{-6}$	511	3.071	175	152	0.2603	26.03
	$7x10^{-6}$	513	3.050	176	163	0.2654	26.54
	$9x10^{-6}$	517	2.494	164	154	0.3993	39.93
	$11x10^{-6}$	523	1.911	173	153	0.5397	53.97
II	$5x10^{-6}$	524	3.082	162	172	0.2577	25.77
	$7x10^{-6}$	527	3.082	169	173	0.2622	26.22
	$9x10^{-6}$	531	2.513	159	154	0.3947	39.47
	$11x10^{-6}$	538	1.974	168	176	0.5224	52.24
III	$5x10^{-6}$	527	3.095	179	154	0.2545	25.45
	$7x10^{-6}$	521	3.078	191	176	0.2586	25.86
	$9x10^{-6}$	528	2.716	174	157	0.3458	34.58
	$11x10^{-6}$	531	2.118	172	148	0.4898	48.98
IV	$5x10^{-6}$	521	3.109	169	138	0.2512	25.12
	$7x10^{-6}$	527	3.099	183	162	0.2536	25.36
	$9x10^{-6}$	536	3.825	176	147	0.3196	31.96
	$11x10^{-6}$	531	2.327	181	151	0.4395	43.95
V	$5x10^{-6}$	524	3.199	172	162	0.2295	22.95
	$7x10^{-6}$	531	3.109	167	138	0.2512	25.12
	$9x10^{-6}$	534	2.917	146	157	0.2974	29.74
	$11x10^{-6}$	546	2.511	138	153	0.3952	39.52
VI	$5x10^{-6}$	519	3.209	171	162	0.2271	22.71
	$7x10^{-6}$	521	3.153	152	181	0.2406	24.06
	$9x10^{-6}$	517	3.102	161	181	0.2528	25.28
	$11x10^{-6}$	524	2.716	148	177	0.3458	34.58

3.2. Potentiodynamic Anodic Measurements (Pitting Corrosion)

The passive film formed spontaneously on austenitic C-steel has been widely studied using surface analysis techniques [20-22]. A mixture of iron and chromium oxides is formed, with hydroxide and H_2O-containing compounds concentrated in the outermost region of the film and chromium oxide enrichment in the inner region (metal/film interface). Thus the passive film formed on the C-steel surface consists of an inner Cr (III)-oxide/hydroxide layer and a very thin outer layer of Fe (II)/(III)-oxide/hydroxide [23].

The effect of adding different concentrations of the studied compounds on the pitting corrosion behavior of C- steel in 0.1 NaCl solution was investigated by potentiodynamic polarization measurements. The addition of the inhibitors increases the breakdown potential towards more positive potential Fig. (4), i.e. inhibits pitting corrosion of the C-steel.

Fig. (5) shows the relation between Epit and the inhibitors concentrations, straight lines obtained according to the following equation:

$$E_{pit} = a' + b' \log [inh.] \quad (3)$$

Symbols a' and b' are constants. The increase of the inhibitors concentration increases the pitting potential to more positive values, i.e. decreases the pitting corrosion. The adsorption of the inhibitors on the C-steel surface can prevent the adsorption of Cl^- ion (which is responsible for pitting corrosion). Pitting potentials; the order of decreasing Epit of C-steel in the presence of the studied compounds is agree with the order of decreasing % IE of these compounds, obtained from Galvanostatic polarization measurements.

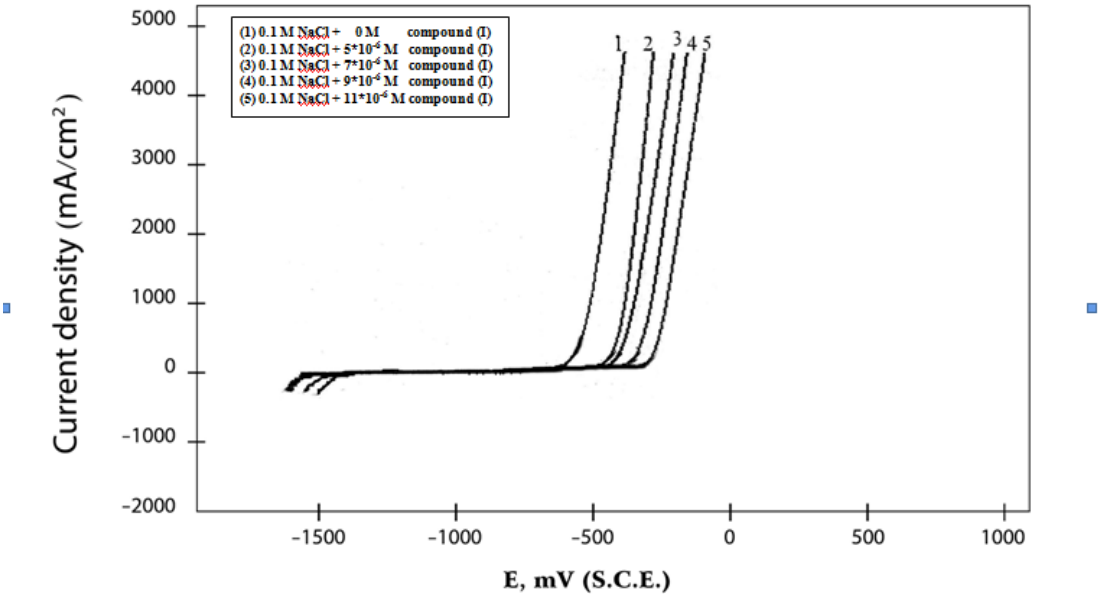

Fig (4): Potentiodynamic anodic polarization curves of C-steel in 0.1 M NaCl containing different concentration of compounds (I)

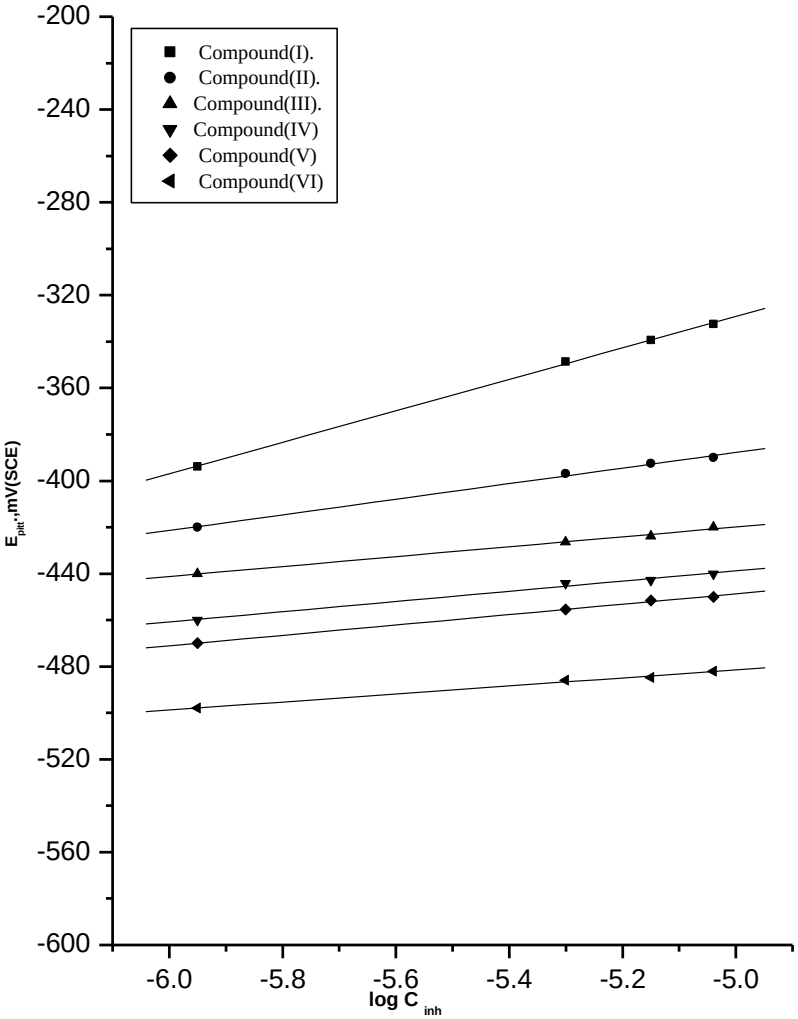

Fig(5):The relationship between pitting potential of C-Steel and logarithm the

3.3. Weight Loss Measurements

Weight-loss of C-steel was determined, using equation (3), at various time intervals in absence and presence of different concentrations of organic derivatives, derivatives (I-VI). The obtained weight loss-time curves are represented in Fig. (6) for inhibitor (I), the most effective one. Similar curves were obtained for other inhibitors (not shown).

$$\Delta w = (w_1 - w_2)/A \qquad (4)$$

Where Δw is the weight loss in mg per unit area, w_1 and w_2 are the weights of the specimen before and after reaction, respectively, and A is the surface area in cm^2.

The curves obtained in the presence of inhibitors fall significantly below that of free acid. In all cases, the increase in the inhibitor concentration was accompanied by a decrease in weight-loss and an increase in the percentage inhibition. These results lead to the conclusion that, these derivatives under investigation are fairly

efficient as inhibitors for C-steel dissolution in hydrochloric acid solution. Also, the degree of surface coverage (θ) by the inhibitor, calculated from equation (5), would increase by increasing the inhibitor concentration.

$$\theta = 1 - (\Delta W_{inh.} / \Delta W_{free}) \quad (5)$$

Where ΔW_{inh} and ΔW_{free} are the weight losses per unit area in presence and absence of the inhibitor respectively.

In order to get a comparative view, the variation of the inhibition effeciencies (% IE) of the inhibitors with their molar concentrations were calculated according to equation (6); values obtained are summarized in Table (5).

$$\% IE = \theta \times 100 \quad (6)$$

Careful inspection of these results showed that, at the same inhibitor concentration, the order of inhibition efficiencies was as follow:

Series 1: (I) > (II) > (III)
Series 2: (IV) > (V) > (VI)

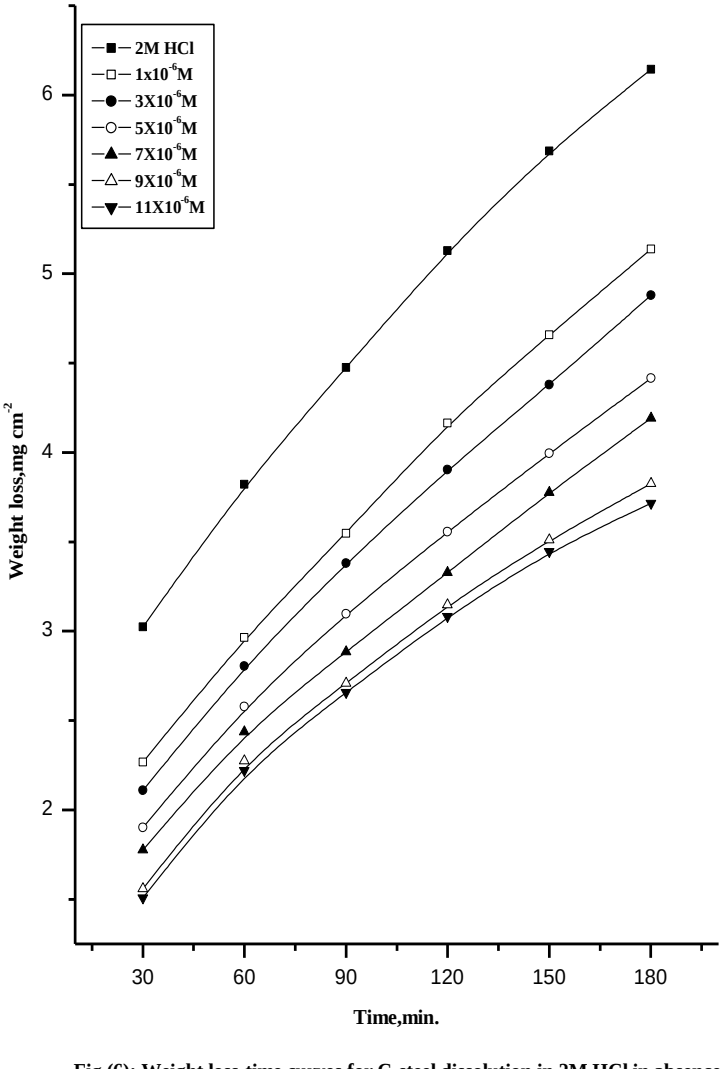

Fig (6): Weight loss-time curves for C-steel dissolution in 2M HCl in absence

Table (5): Inhibition efficiency of all inhibitors at different concentrations of inhibitors as determined from weight loss method for C-steel at 30 °C.

Conc., M.	% IE					
	I	II	III	IV	V	VI
1×10^{-6}	50.55	47.79	46.67	38.14	36.95	36.16
3×10^{-6}	54.49	51.23	50.23	40.17	38.03	35.16
5×10^{-6}	58.28	53.74	51.63	46.71	42.97	41.16
7×10^{-6}	62.41	59.78	58.81	54.49	48.25	45.72
9×10^{-6}	65.31	63.91	62.91	58.31	53.08	49.63
11×10^{-6}	69.21	66.71	65.93	60.82	55.24	51.67

3.4. Synergistic Effect

As seen from Table (5), the percentage inhibition efficiency of the tested derivatives is low, so in order to increase these values we use KI, in addition to the different concentrations of the investigated derivatives. Table (6) shows the % IE of the investigated derivatives in presence of 1×10^{-2} M of KI.

Table (6): Inhibition efficiency at different concentrations of inhibitors in presence of 1×10^{-2} M KI as determined from weight loss method for C-steel at 30 °C.

Conc., M.	% IE					
	I	II	III	IV	V	VI
1×10^{-6}	80.23	79.32	78.28	76.28	73.89	71.63
3×10^{-6}	83.22	82.99	82.66	80.96	78.39	76.23
5×10^{-6}	76.99	86.02	85.99	83.68	81.34	79.33
7×10^{-6}	91.04	91.03	90.98	88.09	85.78	83.53
9×10^{-6}	94.33	93.97	93.68	89.32	88.68	85.82
11×10^{-6}	99.56	97.31	96.30	93.56	90.56	88.07

It can be seen from Table (6) that the addition 10^{-2} M of KI inhibits the corrosion of C-steel to a large extent and by increasing the concentration of organic derivatives (1×10^{-6} -11×10^{-6} M) the percentage inhibition increases. This can be interpreted according to Schmitt and Bedbur [24], which proposed two types of joint adsorption namely competitive and cooperative. In competitive adsorption, the anions and cations are adsorbed at different sites on the electrode surface, and in case of cooperative adsorption, the anions are chemisorbed on the electrode surface and the cations are adsorbed on a layer of the anion, apart from the adsorption on the surface directly.

From the data of Table (6) it is seen that KI would be considered as one of the effective anions for synergistic action. The net increment of inhibition efficiency shows a synergistic effect of KI with organic derivatives. The synergistic effect depends on the type and concentration of anions. The experimental results suggested that the

presence of this anion (I^-) in the solution stabilizes the adsorption of derivatives on the metal surface and improved the inhibition efficiency of these derivatives [25].

Fig. (7). Demonstrates the weight-loss time curves for the dissolution C-steel in 2 M HCl in absence and presence of different concentrations of compound (I) without and with addition of 10^{-2} M KI at 30 ^{o}C.

$$S_\theta = (1 - \theta_{1+2}) / (1 - \theta`_{1+2}) \quad (7)$$

Where $\theta_{1+2} = \theta_1 + \theta_2 - \theta_1 \theta_2$

θ`1+2 Measured surface coverage by the anion in combination with cation. θ_1 and θ_2 are the surface coverage for anions and cations, respectively.

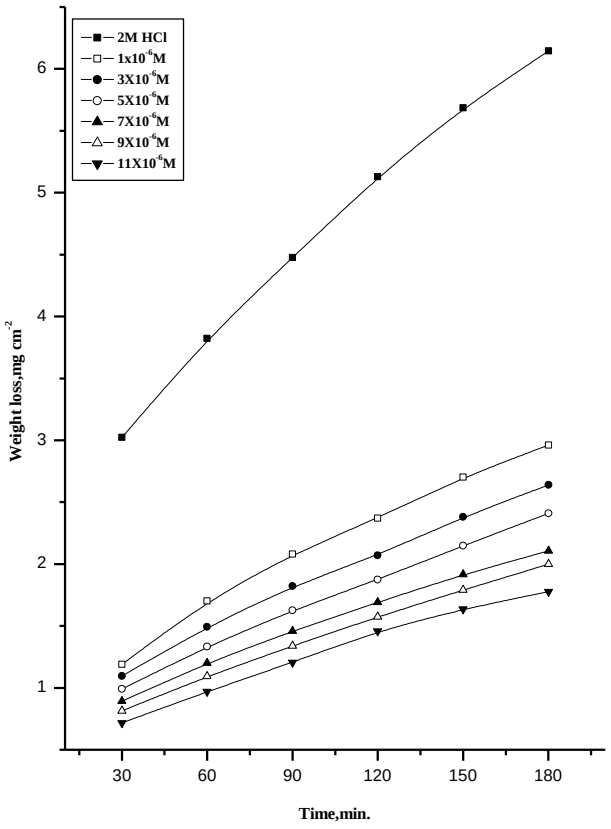

Fig.(7): Weight loss-time curves for C-steel dissolution in 2M HCl in absence

Table (7) lists the variation of the synergistic parameter (S_θ) in the presence of different concentrations of derivatives. It is seen that all values of (S_θ) are less than unity and, therefore, the adsorption of each compound antagonizes the other's adsorption. Thus, derivatives significantly improved the coverage and thus the quality and inhibition efficiency of derivatives on the corroding C-steel.

Derivatives are nitrogen organic derivatives, which contain unshared electron pairs. In strong acidic solutions these derivatives may be protonated, leading to positive charge in molecule. It is also known that C-steel surface has positive charge due to (E_{corr} - E_q = 0),thus it is difficult for the positively charged derivatives to approach the

positively charged C-steel surface ,due to the electrostatic repulsion ,this is why these derivatives cannot act as excellent inhibitors for C-steel corrosion in 2 M HCl solution without containing anions .In case of presence I^- ions, this anion adsorbed on C-steel surface and makes the surface negatively charged by means of electrostatic attraction, after that, protonated organic derivatives are easily reached the surface of C-steel.

Table (7): Synergism parameter (S_θ) at different concentrations of inhibitors as determined by weight loss method for C-steel in 2 M HCl in presence of 1×10^{-2} M KI at 30 °C.

Conc., M.	S_θ					
	I	II	III	IV	V	VI
1×10^{-6}	0.926	0.917	0.935	0.964	0.946	0.947
3×10^{-6}	0.995	0.995	0.958	0.968	0.997	1.012
5×10^{-6}	0.996	0.963	0.934	0.961	0.968	1.043
7×10^{-6}	1.032	1.023	0.986	1.032	1.044	1.023
9×10^{-6}	1.044	1.032	1.025	1.046	1.082	1.054
11×10^{-6}	1.106	1.056	1.074	1.123	1.153	1.340

3.4. Adsorption Isotherm

Organic molecules inhibit the corrosion process by the adsorption on metal surface. Theoretically, the adsorption process can be regarded as a single substitutional process in which an inhibitor molecule (Inh.) in the aqueous phase substitutes an "**x**" number of water molecules adsorbed on the metal surface [26] vis,.

$$Inh._{(aq.)} + xH_2O_{(sur)} \longrightarrow Inh._{(sur.)} + xH_2O_{(aq.)} \quad (8)$$

Where **x** is known as the size ratio and simply equals the number of adsorbed water molecules replaced by a single inhibitor molecule. The adsorption depends on the structure of the inhibitor, the type of the metal and the nature of its surface, the nature of the corrosion medium and its pH value, the temperature, and the electrochemical potential of the metal-solution interface. Also, the adsorption provides information about the interaction among the adsorbed molecules themselves as well as their interaction with the metal surface. Actually an adsorbed molecule may make the surface more difficult or less difficult for another molecule to become attached to a neighboring site and multilayer adsorption may take place. There may be more or less than one inhibitor molecule per surface site. Finally, various surface sites could have varying degrees of activation. For these reasons a number of mathematical adsorption isotherm expressions have been developed to take into consideration some of non-ideal effects.

Adsorption isotherm equations are generally of the form [27]:

$$f(\theta, x) \exp(-a, \theta) = KC \quad (9)$$

Where f (θ, x) is the configurational factor that depends essentially on the physical model and assumptions underlying the derivation of the isotherm, (a) is a molecular interaction parameter depending upon molecular interactions in the adsorption layer and the degree of heterogeneity of the surface; it is a measure of steepness of adsorption isotherm; the more positive the value of (a) the steeper the adsorption isotherm, θ is the degree of surface coverage, C is the inhibitor concentration in the bulk of solution; K is the equilibrium constant of the adsorption process, which is related to the standard free energy of adsorption (ΔG° ads.) by:

$$K = 1/55.5 \exp(-\Delta G^\circ_{ads.} / RT) \quad (10)$$

Where R is the universal gas constant and T is the absolute temperature.

A number of mathematical relationships for the adsorption isotherms have been suggested to fit the experiment data of the present work. The Frumkin's adsorption isotherm [28] is given by the following equation:

$$K C = \theta / 1 - \theta \exp(-2 a \theta) \quad (11)$$

Where K is the equilibrium constant of the adsorption reaction, C is the inhibitor concentration in the bulk of the solution, and θ is the surface coverage. The surface coverage, i.e., the fraction of the surface covered by the inhibitor molecules.

Plots of θ vs. log C (Frumkin adsorption plots) for adsorption of the used inhibitors on the surface of C-steel in 2 M HCl acid solutions at 30°C are shown in Fig. (8). The data gave S-shape indicating that Frumkin's isotherm is valid for these systems.

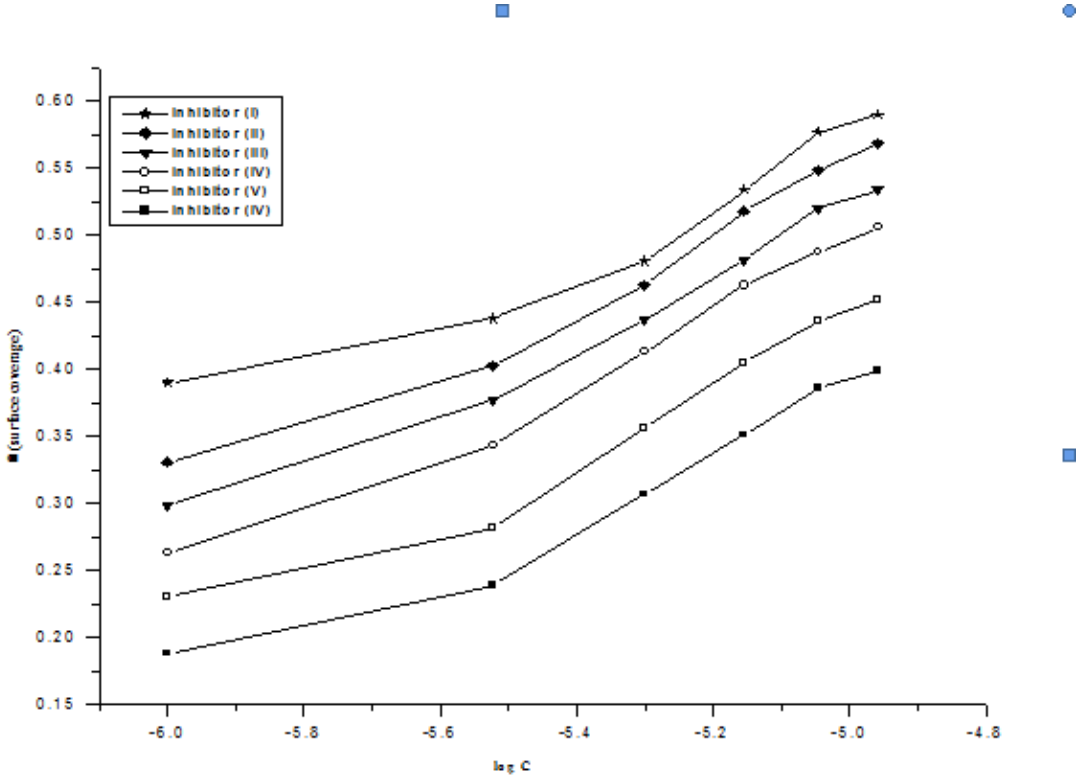

Fig. (8): θ-log C curves for C-steet dissolution in 2 M HCl in presence of different inhibitors from weight loss measurements at 30 °C

The effect of temperature (30–60°C) on the performance of the inhibitors at different concentrations of (1×10^{-6} -11×10^{-6} M) for C-steel in 2 M HCl was studied using weight-loss measurements. Plot of logk (corrosion rate) against 1/T (absolute temperature) Fig. (9) for C -steel in 2 M HCl, gave straight lines. The values of the slopes obtained at different temperatures permit the calculation of Arrhenius activation energy (Ea*). Kinetic parameters for corrosion of C-steel were calculated from Arrhenius-type plot.

$$k=A \exp(-Ea^* / RT) \quad (12)$$

and transition state- type equation :

$$k = RT / Nh \exp(\Delta S^*/R) \exp(-\Delta H^* / RT) \quad (13)$$

The relation between log k/T vs. 1/T gives straight line, from its slope, ΔH* can be computed and from its intercept ΔS* can be also computed Fig. (10).

Table (8) exhibits the values of apparent activation energy Ea*, enthalpies ΔH* and entropies ΔS* for C-steel dissolution in 2M HCl solution. The presence of organic derivatives increases the activation energies of C- steel indicating strong adsorption of the organic molecules on the metal surface and the presence of these additives induces energy barrier for the corrosion reaction and this barrier increases with increasing the additive concentrations.

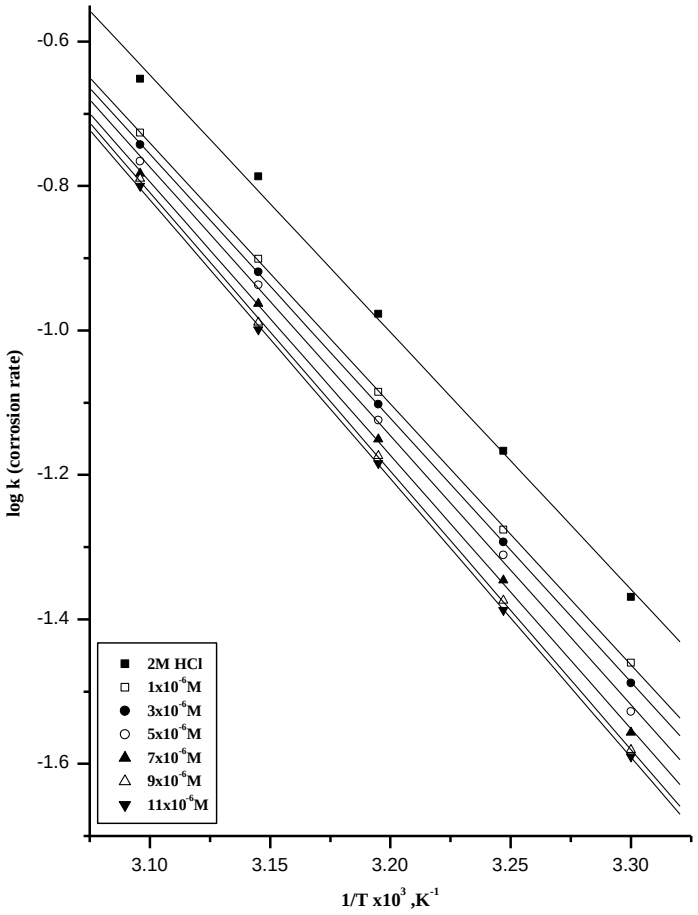

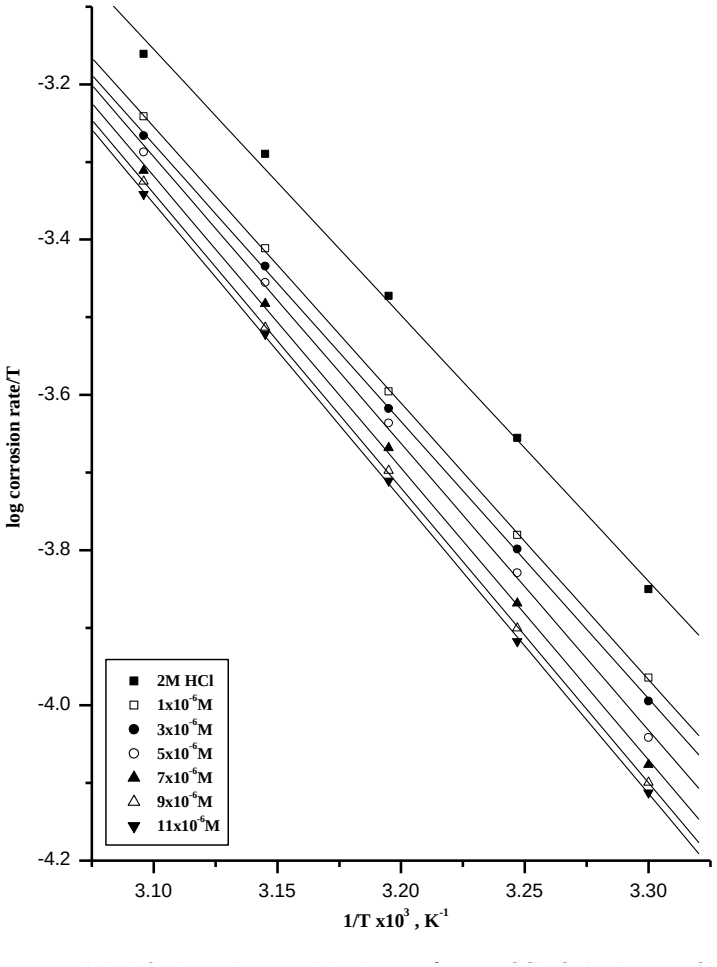

Table (8): Activation parameters for the dissolution of C-steel in presence and absence of different concentrations of inhibitors in 2 M HCl

Inhibitor	Conc., M.	Activation Parameters		
		E_a^*	ΔH^*	$-\Delta S^*$
		kJ mol^{-1}	kJ mol^{-1}	J mol^{-1} K^{-1}
Free Acid (2 M HCl)	0	62.19	60.55	51.66
(I)	1×10^{-6}	71.67	69.02	42.20
	3×10^{-6}	73.92	71.29	36.40
	5×10^{-6}	75.51	72.88	31.85
	7×10^{-6}	78.28	75.64	23.62
	9×10^{-6}	80.27	77.63	17.80
	11×10^{-6}	80.85	78.20	16.30
(II)	1×10^{-6}	70.65	68.02	45.80
	3×10^{-6}	72.80	70.15	37.30

	5×10^{-6}	75.13	72.87	32.00
	7×10^{-6}	76.98	74.32	27.52
	9×10^{-6}	78.91	76.27	21.84
	11×10^{-6}	79.31	76.65	20.94
(III)	1×10^{-6}	70.36	67.70	46.30
	3×10^{-6}	72.77	70.13	39.20
	5×10^{-6}	75.07	72.44	32.46
	7×10^{-6}	76.52	73.87	28.50
	9×10^{-6}	77.41	74.78	26.26
	11×10^{-6}	77.74	75.10	25.33
(IV)	1×10^{-6}	70.11	67.47	46.77
	3×10^{-6}	72.01	69.38	41.34
	5×10^{-6}	74.40	71.77	34.26
	7×10^{-6}	75.71	73.07	30.70
	9×10^{-6}	76.82	74.18	27.63
	11×10^{-6}	77.03	74.47	27.10
(V)	1×10^{-6}	69.75	67.11	47.55
	3×10^{-6}	69.95	67.31	47.37
	5×10^{-6}	72.31	69.67	40.40
	7×10^{-6}	73.58	70.93	36.92
	9×10^{-6}	74.27	71.62	35.24
	11×10^{-6}	74.38	71.75	35.12
(VI)	1×10^{-6}	67.18	65.52	52.31
	3×10^{-6}	68.18	66.34	50.15
	5×10^{-6}	68.90	67.63	46.47
	7×10^{-6}	70.28	68.85	43.06
	9×10^{-6}	71.50	70.19	39.23
	11×10^{-6}	72.84	69.25	40.21

3.6. Quantum Chemical Calculation

The results obtained from the relation between inhibition characteristics and quantum chemical data show that log i_{corr} mostly depends upon the energies of the highest occupied molecular orbital (HOMO) and the lowest unoccupied molecular orbital (LUMO). From Fig. (11) it is evident that the inhibition efficiency increases with the increase of energy of the HOMO, that is, the increase of the ionization potential. It is further evident that the inhibition efficiency increases with the decrease of ionization of the molecule, which means that the molecule acts as an electron donor when blocking the corrosion reaction. The results of Table (9) are calculated at 11×10^{-6} and show that the energies of HOMO orbital of the Thiazolidin-5-one derivatives decrease in the following order:

Series Two: (IV) > (V) > (VI)

Table (9): Quantum chemical parameters of the Thiazolidin-5-one derivatives

Inhibitor	Log i_{corr}	Atom	Charge Density	HOMO Energy Kcal/mole	LUMO Energy Kcal/mole	% Inh.
(IV)	4.0738	S (1) N (2) N (3) O (5) N (13)	+0.072 -0.009 +0.295 -0.238 -0.086	-8.09622	-1.61218	69.03
(V)	6.0534	S (1) N (2) N (3) O (5) O (12)	+0.078 -0.004 +0.296 -0.239 -0.271	-8.16687	-1.70948	60.30
(VI)	6.2086	S (1) N (2) N (3) O (5)	+0.068 -0.019 +0.189 -0.237	-8.36825	-0.77532	59.70

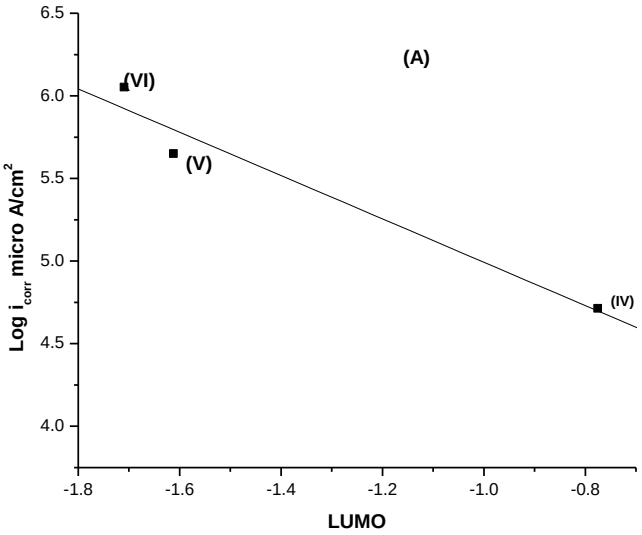

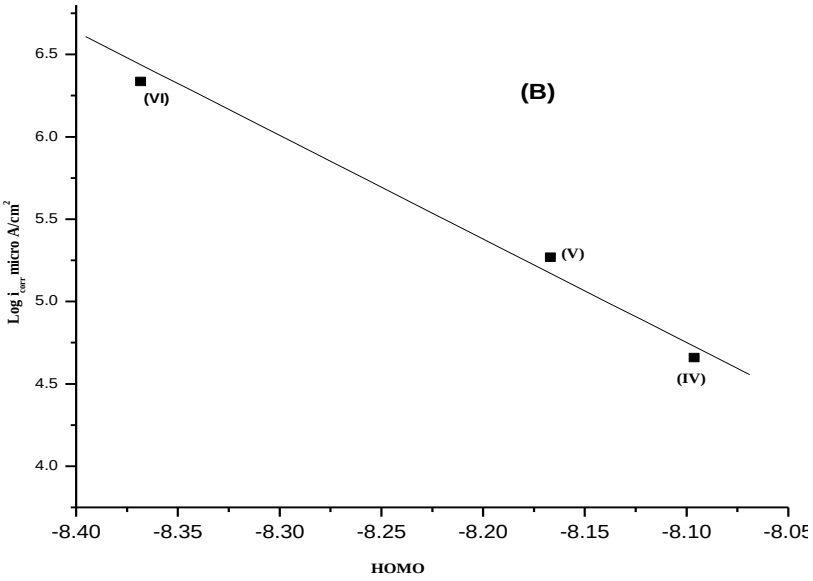

Fig.(11): Correlation of LUMO (A) and HOMO (B) energies with log i_{corr} forthe investigated compounds

3.7. Mechanism of Inhibition

The corrosion inhibition is due to adsorption of the inhibitors at the electrode/ solution interface, the extent of adsorption of an inhibitor depends on the nature of the metal, the mode of adsorption of the inhibitor and the surface conditions. Adsorption on C-steel surface is assumed to take place mainly through the active centers attached to the inhibitor and would depend on their charge density. Transfer of lone pairs of electrons on the nitrogen atoms to the C-steel surface to form a coordinate type of linkage is favored by the presence of a vacant orbital in iron atom of low energy. Polar character of substituents in the changing part of the inhibitor molecule seems to have a prominent effect on the electron charge density of the molecule.

It was concluded that the mode of adsorption depends on the affinity of the metal towards the π-electron clouds of the ring system. Metals such as Cu and Fe, which have a greater affinity towards aromatic moieties, were found to adsorb benzene rings in a flat orientation. The order of decreasing the percentage inhibition efficiency of the investigated inhibitors in the corrosive solution was as follow**:**

- **For Series One: (I) > (II) > (III):**

Compound (I) exhibits excellent inhibition power due to: (i) its larger molecular size (418) that may facilitate better surface coverage, (ii) its adsorption through five active centers as shown from Fig. (12), and (iii) the presence of p-CH_3 (σ = -0.17) which is highly electron releasing group which enhance the delocalized π-electrons on the active centers of the compound.

Compound (II) comes after compound (I) in inhibition efficiency inspite of it has five active centers, because it has lesser molecular size (414) and has no substituent in p-position (H-atom with σ =0.0) which contributes no charge density to the molecule.

Compound (III) has the lowest inhibition efficiency. This is due to it has four active centers and the lowest molecular size (308).

- **For Series Two: (IV) > (V) > (VI):**

Compound (IV) exhibits excellent inhibition power due to: (i) its larger molecular size (399) that may facilitate better surface coverage, and (ii) its adsorption through three active centers as shown from Fig (3.123).

Compound (V) comes after compound (IV) in inhibition efficiency inspite of it has three active centers, but it has lower molecular size (372).

Compound (VI) has the lowest inhibition efficiency. This is due to it has the lowest molecular size (268) and it has only two active centers**.**

Series One

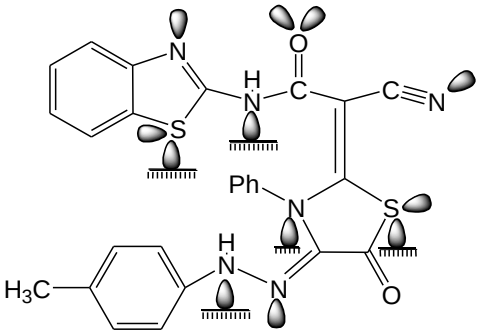

(I)

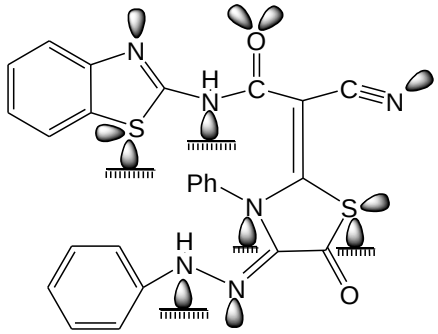

(II)

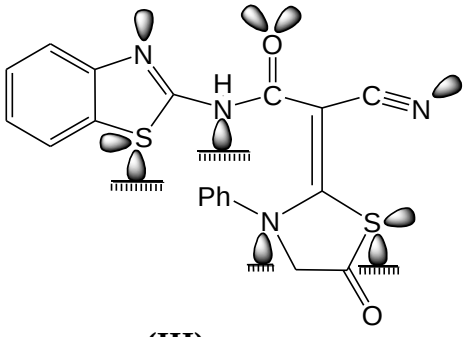

(III)

Series Two

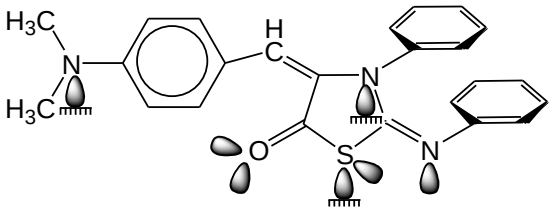

(IV)

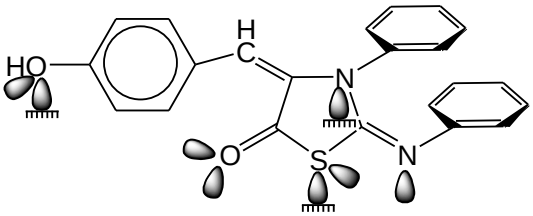

(V)

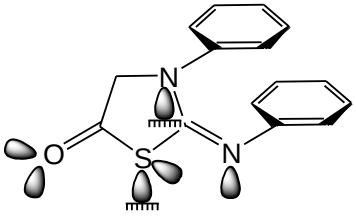

(VI)

References

[1] Z. Wahbi, A. Guenbour, H. Abou El Makarim, A. Ben Bachir, S. El Hajjaji, Porg.Org. Coat. 60 (2007) 224.
[2] K.F. Khaled, Electrochim. Acta 53 (2008) 3484.
[3] K.F. Khaled, Appl. Surf. Sci. 252 (2006) 4120.
[4] M.A. Amin, S.S. Abd El Rehim, H.T.M. Abdel-Fatah, Corros. Sci. 51 (2009) 882.
[5] S.S. Abdel Rehim, O.A. Hazzazi, M.A. Amin, K.F. Khaled, Corros. Sci. 50 (2008) 2258.
[6] H.H. Hassan, E. Abdelghani, M.A. Amin, Electrochim. Acta 52 (2007) 6359.
[7] M.A. Amin, S.S. Abd El Rehim, E.E.F. El-Sherbini, R.S. Bayoumi, Electrochim. Acta 52 (2007) 3588.
[8] K.F. Khaled, M.A. Amin, Corros. Sci. 51 (2009) 1964.
[9] M. Ozcan, F. Karadag˘, _I. Dehri, Colloid Surface A 316 (2008) 55.
[10] E.E. Oguzie, Y. Li, F.H. Wang, Electrochim. Acta 53 (2007) 909.
[11] E.E. Oguzie, Y. Li, F.H. Wang, J. Colloid and Interf. Sci. 310 (2007) 90.
[12] A.B. Silva, S.M.L. Agostinho, O.E. Barcia, G.G.O. Cordeiro, E. D'Elia, Corros. Sci. 48 (2006) 3668.
[13] O. Olivares, N.V. Likhanova, B. Gomez, J. Navarrete, M.E. Llanos-Serrano, E.Arce, J.M. Hallen, Appl. Surf. Sci. 252 (2006) 2894.
[14] K.F. Khaled, M.A. Amin, Corros. Sci. 51 (2009) 2098.
[15] K.F. Khaled, Mat. Chem. Phys. 112 (2008) 104.
[16] K.F. Khaled, M.A. Amin, J. Appl. Electrochem. 38 (2008) 1609.
[17] K.F. Khaled, Electrochim. Acta 54 (2009) 4345.
[18] M.A.Metwally,E.M.keshk anda.fekry:phosphorus,sulfur and Silicon and the related elements., 179 (2004) 2067.
[19] George E. Dieter, Mechanical Metallurgy, University of Maryland, (1988).
[20] J.L. Polo, E. Cano and J.M. Bastidas; J. Electroanal. Chem.; 537 (2002) 183
[21] C.M. Abreu, M.J. Cristo´bal, X.R. No´voa, G. Pena and M.C. Pe´rez; Electrochim. Acta; 49 (2004) 3049.
[22] S.S. El-Egamy and W.A. Badaway; J. Appl. Electrochem.; 34 (2004) 1153
[23] N.P. Cosman, K. Fatih and S.G. Roscoe; J. Electroanal. Chem.; 574 (2005) 261
[24] G.Schmilt, K.Bedbur and Ü.Korros. 36 (1985) 237.
[25]E. Khamis, E.S.H. El- Ashry, and A.K. Ibrahim ., Br. Corros., 2 (2000)35.
[26] G.B. Ateya, B. El-Anadouli, and F. El-Nizamy, Corros. Sci., 24 (1984) 509.
[27] E. Khamis, M.A. Ameer, N.M. Al-Andis, and G. Al-Senani, Corrosion, 56 (2) (2000) 127.
[28] K. Haladky, L.Collow and J.Dawson, Br.Corros. J.,15 (1980) 20.
[29] J. N. Wanklyn; Corros. Sci., 21 (1981) 211.
[30] M. A. A. Tullmin and F. P. A. Robinson; Corrosion; 44 (1988) 664.
[31] W. R. Ciesak and D. J. Duquette; J. Electrochem. Soc.,132 (1985) 533.
[32] J. R. Galvole, J. B. Lumsden and R. W. Stechle; J. Electrochem. Soc., 125 (1978) 1204.
[33] K. Sugimoto and Y. Sawada; Corrosion; 32 (1976) 347.